Transaction B: Mechanical Engineering
Vol. 17, No. 2, pp. 136–145

SCIENTIA IRANICA

Effects of Canard Position on Wing Surface Pressure

M.R. Soltani[1,*], F. Askari[1], A.R. Davari[2] and A. Nayebzadeh[1]

Abstract. *A series of wind tunnel tests were performed to study the effects of a canard and its position on the downstream flowfield over the wing surface. The wing surface pressure was measured for both canard-off and canard-on configurations. In addition, the canard position effects on the wing were investigated at different angles of attack. The canard was installed at three vertical positions and at two different horizontal distances from the wing apex. The results show a remarkable increase in the wing suction peak for the canard-on configurations. At low to moderate angles of attack, among the various configurations examined in the present experiments, the mid-canard configuration developed a higher suction on the wing while, at high angles of attack, the upper-canard was found to induce the most favorable flow field on the wing. In addition, higher suctions were achieved on the wing at moderate to high angles of attack, as the wing-canard distance was increased.*

Keywords: *Canard; Delta wing; Downwash; Leading edge vortex.*

INTRODUCTION

Canard-wing configurations play an important role in modern fighter aircraft design. High performance aircraft, such as military fighters, often require high-lift for a wide range of angles of attack to maintain their maneuverability. For two-dimensional airfoils, the maximum lift is typically obtained at about 10°-15° angles of attack after which the airfoil stalls. Thus, high performance aircraft require lift enhancement when operating under high angle of attack conditions. One technique for obtaining enhanced lift at moderate angles of attack is through the use of delta-shaped platforms along with strakes. As flow separates along the leading edges of a delta wing at moderate angles of attack, vortical flow results. These vortices produce a very low-pressure region and can account for up to 30% of the total lift at moderate to high angles of attack [1]. A 70° swept delta wing, for example, continues to increase its lift until an angle of attack of about 35° [2]. However, there are some limits to the advantages provided by the delta wing vortices. As the angle of attack is increased, a sudden breakdown in the vortex structure occurs. This phenomenon known as vortex bursting, results in a sudden stagnation of axial flow and an expansion in the vortex radial size [3-5]. Once the vortex structure is diminished, lift starts to decay. Thus, it is desirable for the vortex burst to be delayed as far as possible to get higher lift. Attempts to control delta wing vortices (under static conditions) includes blowing [6,7], suction and the use of canards [8]. The canard induces a non uniform distribution of local angles of attack on the wing surface, which leads to a non conical vortex formation over the wing, and delays the vortex breakdown to higher angles of attack. On the other hand, the wing produces an up-wash field on the canard, which increases its lift. The wing also induces a longitudinal velocity component on the canard. This induced velocity delays the vortex breakdown onset on the canard and increases its performance at moderate to high angles of attack [9,10]. Several investigations have been devoted to studying the flowfield associated with canard-wing configurations. Most of them involve the study of canard shape and deflection angle as well as the body angle of attack on the flowfield. In this paper, a comprehensive survey was performed to underscore the impact of canard and its position on the structure of the flowfield over a delta wing platform.

These results can be generalized to investigate

1. *Department of Aerospace Engineering, Sharif University of Technology, Tehran, P.O. Box 11155-8639, Iran.*
2. *Department of Mechanical and Aerospace Engineering, Islamic Azad University, Science and Research Campus, Tehran, P.O. Box 14155-4933, Iran.*
*. *Corresponding author. E-mail: msoltani@sharif.edu*

Received 20 June 2009; received in revised form 4 October 2009; accepted 12 December 2009

split canard configurations where two canards are used in a tandem arrangement to increase performance and maneuverability. Further, in modern conventional high lift systems, interaction of the forward element on the main body is similar to that observed on the canard-wing model considered in the present experiments.

MODEL AND EXPERIMENTAL APPARATUS

The present experiments were performed in a subsonic wind tunnel. The tunnel is of a closed return type and has a test section with dimensions of 80×80 cm. The maximum attainable speed in the test section is 100 m/sec and the Reynolds number varies between 5.29×10^5 and 5.26×10^6 per meter. Turbulence intensity in the test section has been measured to be less than %0.1.

The investigations have been performed on a canard-wing-body configuration. Figure 1, shows the model installed in the test section. A 60° swept canard is placed in front of the main 60° swept delta wing. The main wing has a constant thickness of 10 mm and is made of aluminum alloy. The wing and canard aspect ratios are 1.17 and 1.15, respectively, and both have a hexagonal profile.

Seventy eight pressure ports of 0.8 mm inner diameter were carefully drilled on the upper surface of the main wing. Figure 2 shows the pressure tabs arrangement on the wing.

Both the wing and the canard were attached to a rectangular cross section fuselage. The model assembly was such that the canard position on the body could be varied in both longitudinal and lateral directions, as shown in Figures 3a through 3f.

The tests were conducted at a constant air speed of 80 m/sec, corresponding to a Reynolds number of 1.480×10^6 based on the wing root chord. The model angle of attack was varied from $-10°$ to $30°$. All data were acquired by an AT-MIO-64E-3 data acquisition

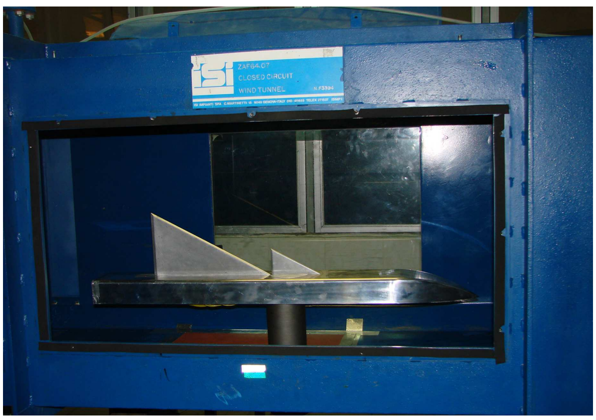

Figure 1. The model installed in the test section.

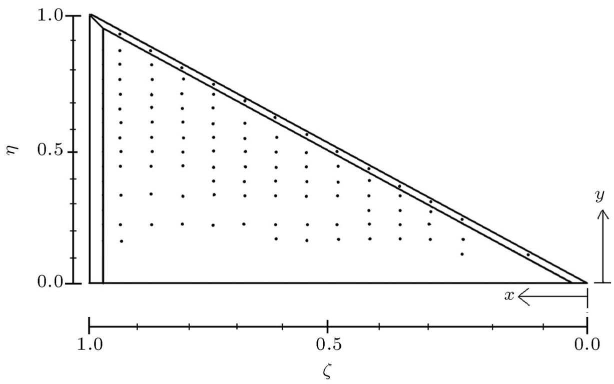

Figure 2. The pressure tabs arrangement on the wing.

board capable of scanning 64 channels at a rate of 500 KHz.

Finally, all data were corrected for the wind tunnel sidewalls and the wake blockage effects. An analytical approach [11] was also used to estimate the errors involved in the pressure measurements. Both the single sample precision and the bias uncertainty in the pressure measurement were estimated. On this basis, the overall uncertainty for the presented data is less than ±3% [12,13].

Results

The results presented in this section are for various cases of canard-on and canard-off configurations. Figure 4 shows the wing surface pressure distribution for both canard-off and canard-on configurations at $\alpha = 10°$, $20°$ and $30°$. The leading-edge vortex signature can be observed from the suction peaks for both configurations. At 10 and 30 degree angles of attack, the wing pressure distribution for the canard-on cases show that the value of the suction peaks for the front sections, $\zeta \leq 0.5$, are higher than the corresponding locations on the canard-off ones, while at the rear sections of the wing, the canard-on surface pressure is obviously higher (Figure 4). Further, it is observed that the wing vortex core for the canard-on configurations lies closer to the wings leading edge than those of the canard-off ones. However, for both configurations, the amount of suction on the wing surface reduces as it moves streamwise from the wing leading edge to the trailing edge. At $\alpha = 30°$, the spanwise pressure is nearly constant on the entire wing surface for the canard-off configuration (an indication of the vortex breakdown) while for the canard-on case, the flow near the leading edge ($\zeta = 0.3$ and $\zeta = 0.4$) is seen to be highly energized by the canard vortical field and a strong suction is developed in this area (Figure 4c).

The above phenomenon can be observed more clearly in Figure 5, where a direct comparison of pressure distributions over the wing is made for the

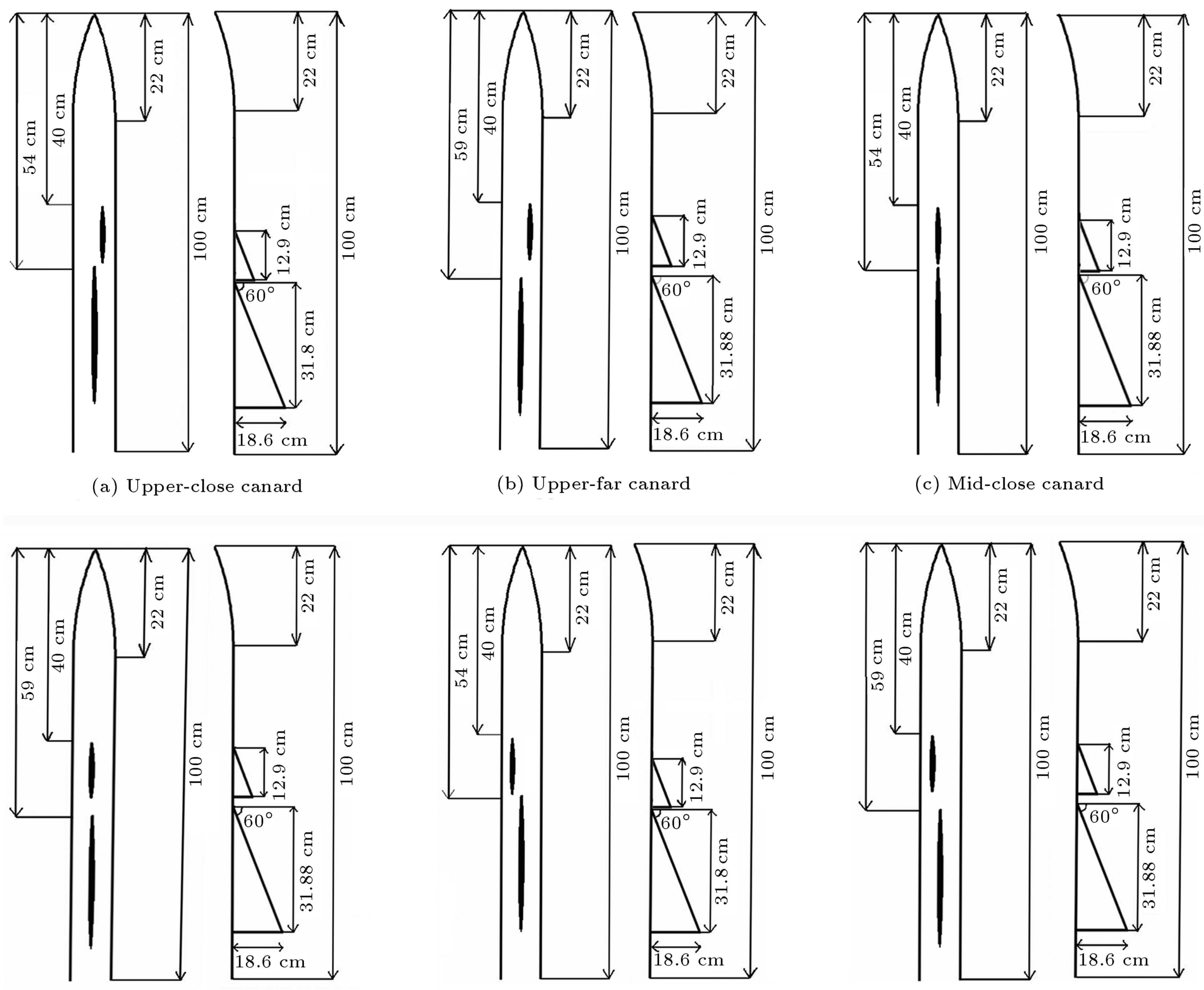

(a) Upper-close canard (b) Upper-far canard (c) Mid-close canard

(d) Mid-far canard (e) Lower-close canard (f) Lower-far canard

Figure 3. Various model configurations.

canard-on and canard-off configurations at $\alpha = 15°$ and 30° and at four different chordwise sections. The suction peak for a 15° angle of attack is nearly sharp, while that for $\alpha = 30°$ is flatter and its value is much lower when compared with the $\alpha = 15°$ case. This is an indication of the vortex burst onset, i.e. at a 30° angle of attack, the vortex on the wing surface bursts; thus, the suction peak has been reduced significantly.

For sections $\zeta = 0.5$ to $\zeta = 0.7$, the suction peak indicates a stronger vortex for the canard-on configurations than that for the canard-off ones. However, as the angle of attack is increased to 30°, it seems that the burst position of the canard vortex reaches the wing surface around $\zeta = 0.7$ and the canard-on suction in this case is less than that of the canard-off (Figure 5). At a farther distance, i.e. $\zeta = 0.8$, the whole spanwise section is exposed to the burst vortex of the canard and the wing.

Quantitatively, at $\zeta = 0.5$, the presence of the canard has enhanced the wing vortex strength by about 150% at $\alpha = 15°$ and 25% at $\alpha = 30°$ in comparison with the canard-off configuration. At $\zeta = 0.7$, the difference between the suction peak values of the wing for the canard-on and canard-off configurations is about 27% at $\alpha = 15°$ and about 14% at $\alpha = 30°$.

Regarding further comparisons with the canard-off cases, the suction peak at all sections on the wing for the canard-on configurations are closer to the leading edge. At $\zeta = 0.8$, the presence of the canard has enhanced the wing vortex strength by about 45% at $\alpha = 15°$, but at $\alpha = 30°$ the vortex strength for both configurations has been decreased and the suction peak for the canard-on configuration is less than that of the canard-off one.

It is well known that the canard induces a downwash field within its span and an upwash field outside its span. The downwash reduces the effective angle of attack considerably in the forward and inner portion of the wing, which leads to a suppression of the flow separation on the wing surface. The upwash field increases the effective angle of attack in the outer and rear portion of the wing, which enhances the flow

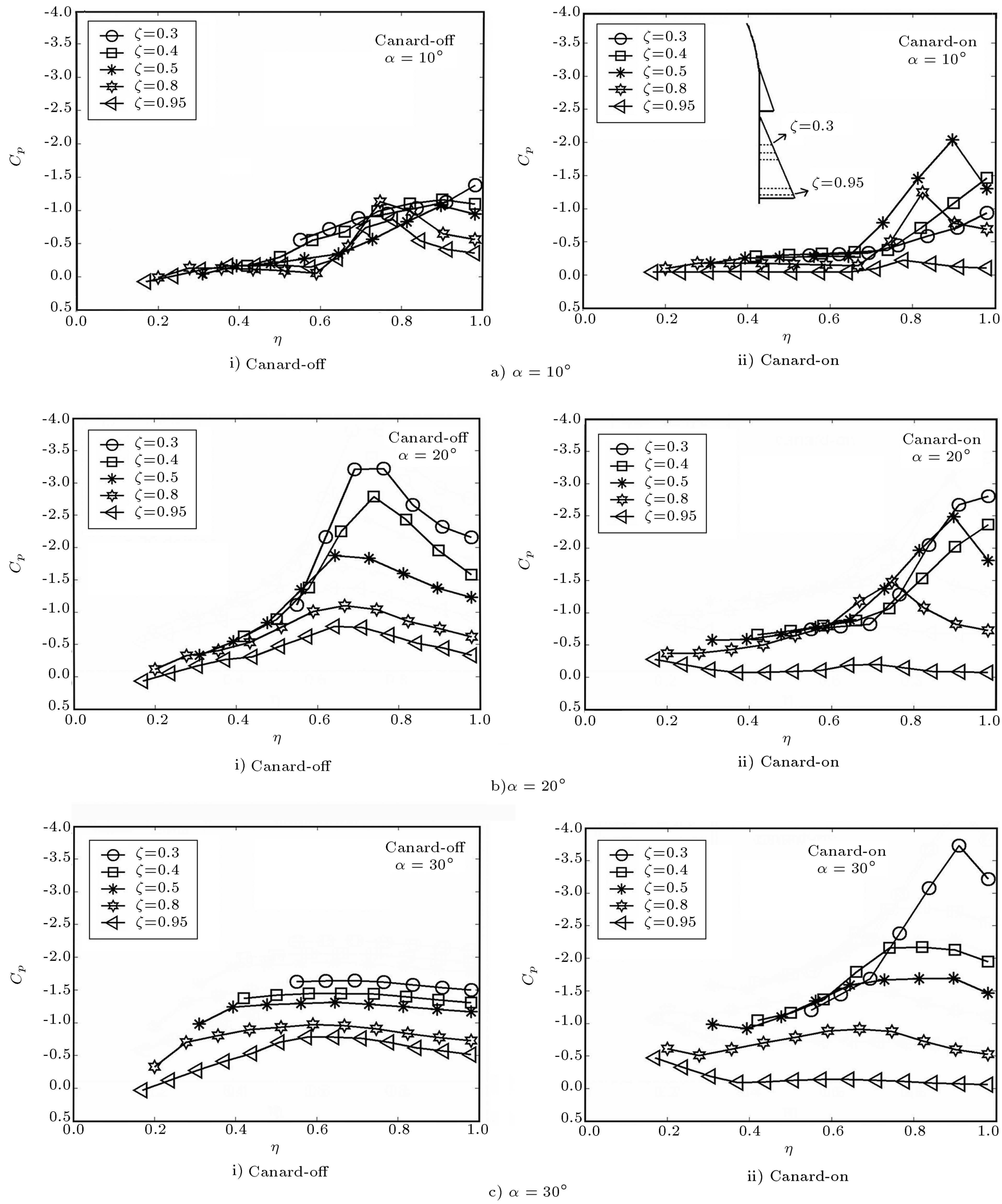

Figure 4. Surface-pressure distribution for several angles of attack at different sections for the mid-close-canard case.

separation there. This mechanism delays the formation of the wing vortex for the canard-on configuration.

Due to the nonuniform distribution of the effective angle of attack along the leading edge of the wing, the wing vortex is fed with vorticity in a different manner than in the case of the canard-off configuration. As a result, the wing for the canard-on configuration sees a lower effective angle of attack and this leads to a compensation of an additional lift of the canard through a loss of lift of the wing. In the rear portion of the wing, near the trailing edge, the magnitude of the suction peak is lower than that of the front part, at all angles of attack. At high angles of attack, however, the suction peak is removed for the canard-

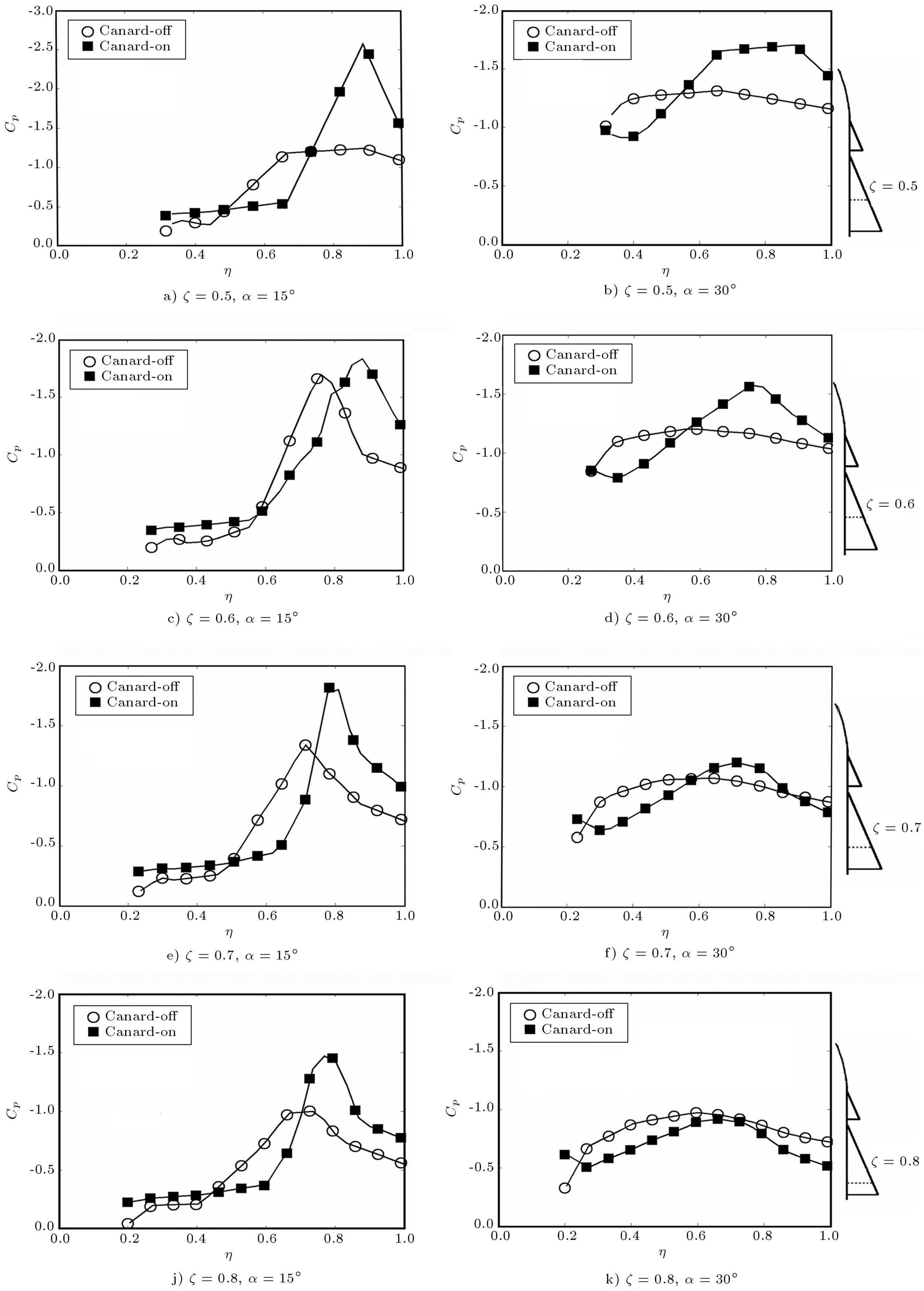

Figure 5. Direct comparison between canard-off and canard-on configuration for the mid-close-canard.

off configuration, at all sections, indicating the vortex breakdown phenomenon.

As observed earlier, for the canard-on configuration, the suction peak on the wing surface pressure at front and middle portions are higher than the corresponding canard-off cases while at the rear portion, the amount of the suction peak for the canard-on configuration has been reduced. This implies that the domain of the favorable influence of the canard is mostly restricted to the front and middle portions of the wing.

Experimental data for the six different wing-canard configurations are shown in Figure 6. The effects of the canard position on the wing surface pressure distribution are clearly seen. For this study, the canard was located at three different vertical positions and at two different horizontal locations. The models are 1-upper close canard, 2-upper-far canard, 3-mid-

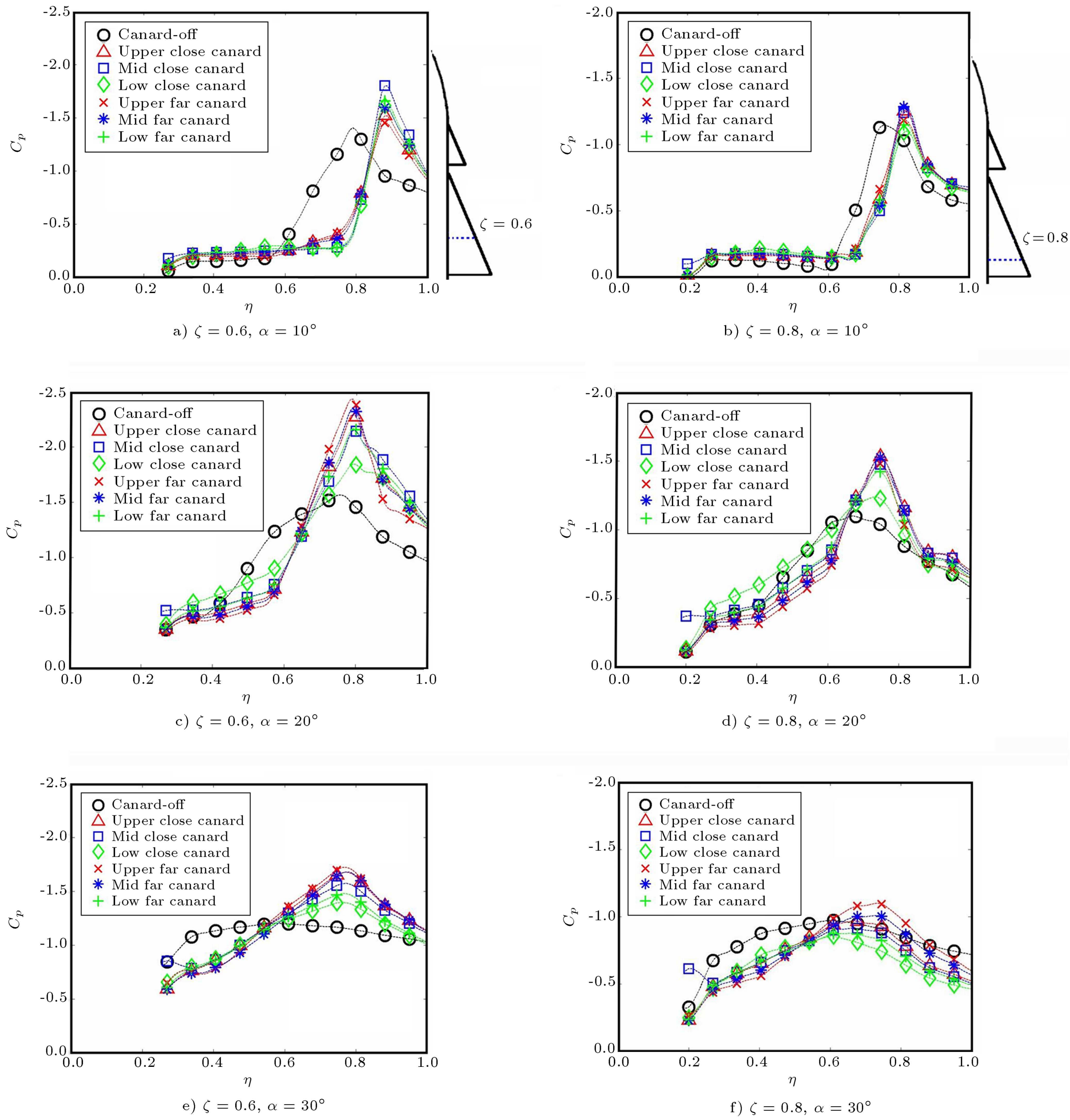

Figure 6. Effect of canard position on the wing pressure distribution.

close canard, 4-mid-far canard, 5-low-close canard and 6-low-far canard. Note that all different configurations are shown in Figure 3. The canard-off data are also shown in each figure for comparison. For the canard-on configurations, the wing surface pressure pattern remains the same, regardless of the canard position. From Figure 6, the difference between the canard-on and canard-off configurations in developing the suction region on the wing surface is clearly evident.

The suction peaks lie closer to the wing leading edge for all canard-on configuration cases. At $\alpha = 10°$ and for $\zeta = 0.6$, the presence of the canard has moved the suction peak toward the wing leading edge, and its value has been increased about 5 to 25 percent, depending on the location of the canard relative to the wing (Figure 6a). At $\zeta = 0.8$ and for the same angle of attack, however, the canard has displaced the suction peak on the wing towards the leading edge by about 7% of the local chord. At $\alpha = 20°$ and for $\zeta = 0.6$ and 0.8, the suction peak movement toward the leading edge, due to presence of the canard, was about 3% to 7% of the local chord, respectively.

Furthermore, from Figure 6 it is clearly seen that for the canard-off cases, the suction peak is much less than for that of the canard-on cases. This phenomenon indicates that the canard not only moves the vortex location over the wing surface, but also increases its strength.

Further comparison of the experimental data shown in Figures 6e and 6f reveals that at high angles of attack, the wing vortex for the canard-off configuration bursts, while for the wing with a canard located upstream, the flowfield has been significantly improved, especially for the $\zeta = 0.6$ case. For $\zeta = 0.8$, Figure 6f shows that at this angle of attack, only for two canard locations, an improvement in the vortical flow is achieved. For other configurations, Figure 6f shows that there still exists a vortex on the wing, due to the canard, however, this vortex is not as strong as those observed in Figures 6a through 6e.

Figure 6 also indicates that among the different canard positions considered here, the up-canard configuration has the strongest and the low-canard has the weakest favorable effect on the wing vortex.

The maximum suction value at different angles of attack for six sections on the wing surface for both canard-off and canard–on cases is shown in Figure 7. According to this figure, the amount of suction on the wing decreases as moving away from the wing apex. At the rear portions of the wing, near the trailing edge, the amount of suction is roughly half that of the front region, $\zeta = 0.4$.

At the front section of the wing, $\zeta = 0.4$, for low to moderate angles of attack, the suction peak for the canard-off configuration is higher than the canard-on case, but, at high angles of attack this phenomenon is reversed. At the middle section of the wing ($\zeta = 0.5$ to 0.8) the suction for most canard-on configurations is higher than that of the canard-off, especially for the mid and up-canard configurations. At the rear portion of the wing, ζ=0.9, the suction peak is reduced significantly for all configurations examined and at all angles of attack, which, as noted earlier, indicates that the canard vortex strength at the rear portion of the wing decreases. As shown in Figure 7, for the mid-canard configuration case, higher suction is achieved at low to moderate angles of attack, and at high angles of attack, at most sections of the wing, the high-canard configuration induces a higher suction peak on the wing surface.

The wing surface pressure contours at different angles of attack for the canard-off and canard-on (upper far canard) configurations are compared in Figure 8. As shown in this figure, a low pressure region over the wing, indicating the presence of the leading edge vortex, is clearly seen, and it is observed that for all cases, the vortex strength near the wing apex is much higher than that in the rear region near the trailing edge. According to this figure, the width of the low pressure region over the wing surface for the canard-on case is smaller than the canard-off one and is aligned closer to the leading edge. The distribution of pressure over the wing at $\alpha = 30°$ indicates that the vortex bursts for the canard-off case, while the suction peak in the pressure distribution for the canard-on case verifies that a vortex does exist at the front portion of the wing.

For the mid-canard configuration and at low angles of attack, the suction peak increases, however, at higher angles of attack, this canard position is not the best (Figure 8). For high angles of attack, the data shows that when the canard is located at its upper position, a remarkable improvement is achieved in the surface pressure pattern. On the other hand, by increasing the longitudinal clearance between the canard and the wing, the absolute value of the suction peak is increased for moderate to high angles of attack. It seems that 'upper and far' is a better position for the canard from among the wing-canard-body configurations examined in this investigation.

CONCLUSION

Extensive low speed wind tunnel tests have been carried out on several wing-canard-body combinations. Surface-pressure results are presented for both canard-off and canard-on configurations. In addition, the effect of canard location on wing surface pressure was investigated. The main results of these investigations are as follows:

1. The downwash of the canard reduces the effective

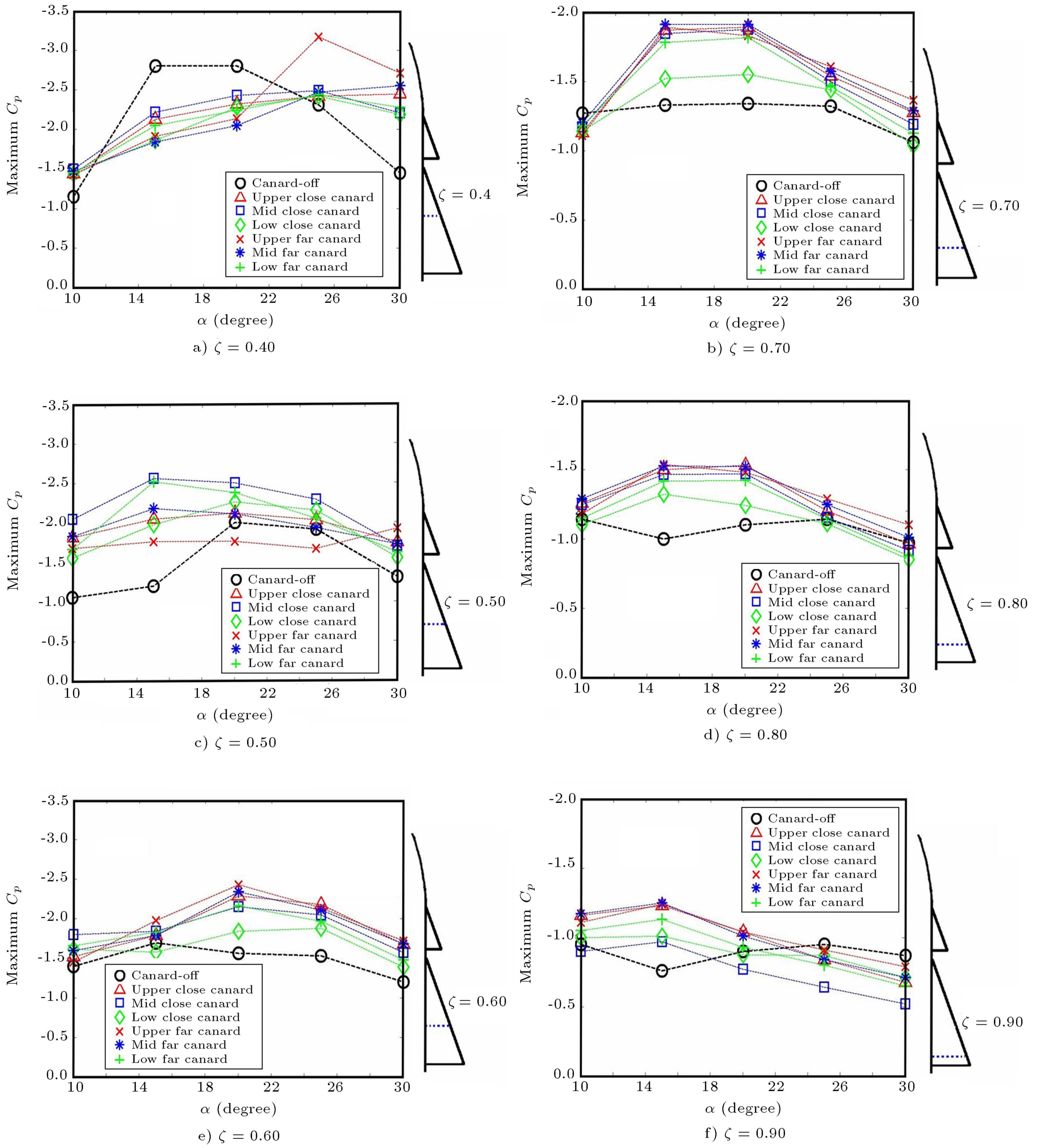

Figure 7. Maximum suction developed at the different sections of the wing.

angle of attack at the inboard section of the wing near the apex. This inhibits flow separation on the wing and, therefore, delays the formation of the leading-edge vortex. At the wing outboard portion, the upwash of the canard separates the flow, forming a side-edge vortex.

2. For the canard-on configurations, a considerably high suction region exists in the front portion of the wing and the suction peaks lie closer to the leading edge when compared with the canard-off cases.

3. For the low-canard configuration, minimum suction is developed on the wing and this configuration is shown to have the least performance among the cases considered. At low angles of attack,

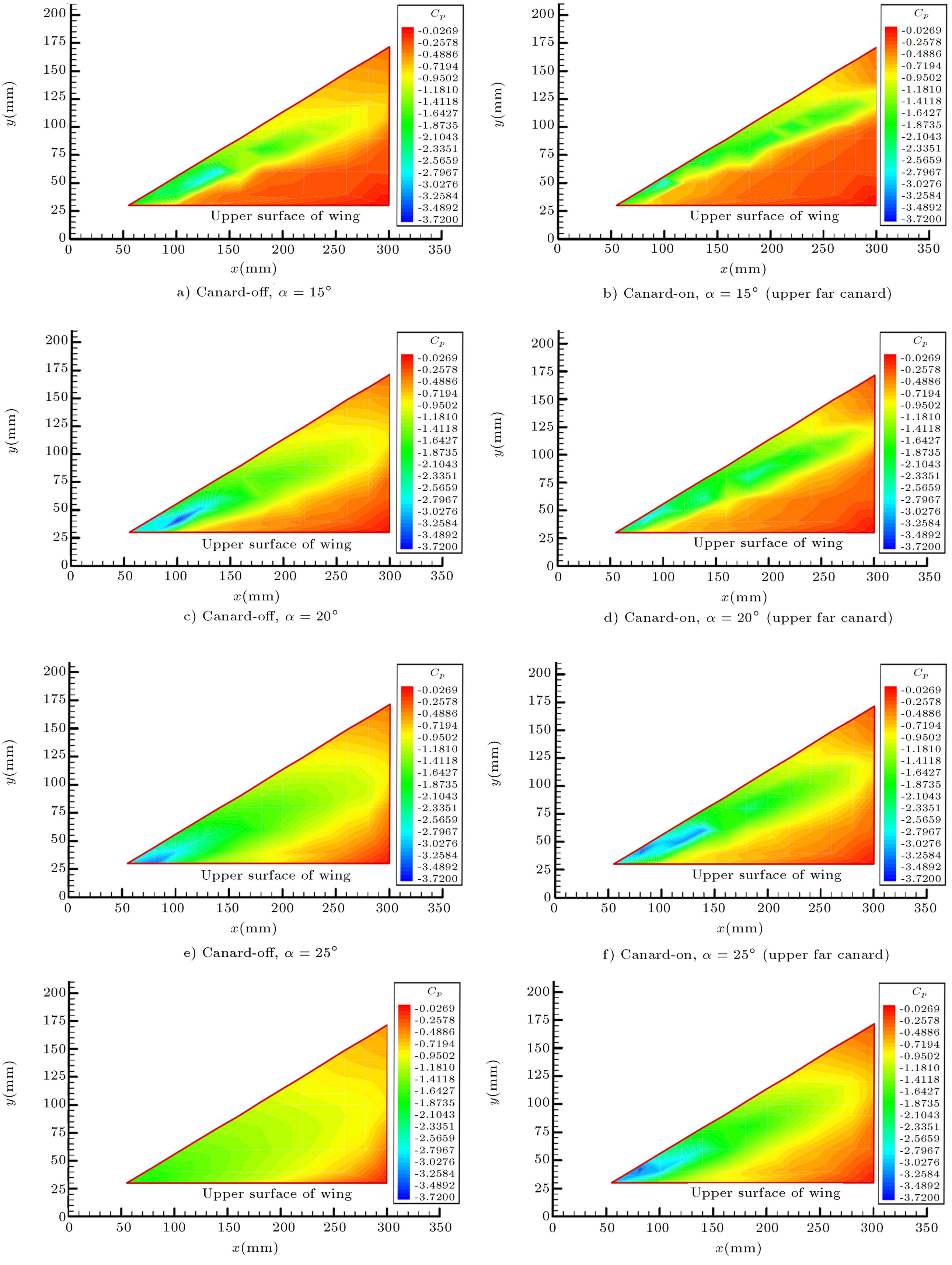

a) Canard-off, $\alpha = 15°$

b) Canard-on, $\alpha = 15°$ (upper far canard)

c) Canard-off, $\alpha = 20°$

d) Canard-on, $\alpha = 20°$ (upper far canard)

e) Canard-off, $\alpha = 25°$

f) Canard-on, $\alpha = 25°$ (upper far canard)

j) Canard-off, $\alpha = 30°$

k) Canard-on, $\alpha = 30°$ (upper far canard)

Figure 8. Pressure distribution over the wing for various angles of attack.

the maximum suction on the wing belongs to the mid-canard configuration, while at higher angles of attack, the high-canard induces the highest suction on the wing.

4. By increasing the horizontal distance between the canard and the wing, higher suction is achieved for moderate to high angles of attack. It seems that the upper far position for the canard is a proper choice for the best performance at high angles from among the wing-canard-body configurations.

ACKNOWLEDGMENT

The work was supported by the AIO and the ADSRC. The authors would like to express their gratitude to the chairman and personnel for their cooperation and support.

NOMENCLATURE

x	chordwise coordinate measured from the wing apex,
y	spanwise coordinate measured from the root,
ζ	local chordwise coordinate along the wing, nondimensionalized by the root chord,
η	local spanwise coordinate along the wing, nondimensionalized by the wing span,
α	model angle of attack,
c_p	static pressure coefficient.

REFERENCES

1. Ashraf, A. Omar, Sri, S. "Experimental investigation of incompressible flow around delta wing-slender body combinations", *International Journal of Applied Engineering Research (IJAER)*, **2**(4), pp. 685–698 (2007)
2. Wei-Jen, S., Curtis, W. "Aerodynamic characterization of a canard guided artillery projectile", *AIAA 2007-672* (2007).
3. Pandya, S.A. and Aftofmis, M.J. "Computation of external aerodynamics for a canard rotor/wing aircraft", *AIAA 2001-0997* (2001).
4. Howard, R.M. and O'Leary, J. "Flow field study of a close-couple canard configuration", *AIAA Journal*, **31**(4), pp. 908-914 (1994).
5. Earnshaw, P.B. and Lawford, I.A. "Low-speed wind tunnel experiments on a series of sharp-edged delta wings", *Aeronautical Research Council*, RM 3424 (1964).
6. Erickson, G.E. "Water-tunnel studies of leading-edge vortices", *Journal of Aircraft*, **19**(6), pp. 442-448 (1982).
7. Seginer, A. and Salomon, M. "Performance augmentation of a 60-degree delta aircraft configuration by spanwise blowing", *Journal of Aircraft*, **23**(2), pp. 801-807 (1986).
8. Wood, N.I. and Roberts, L. "Control of vortical lift on delta wings by tangential leading-edge blowing", *Journal of Aircraft*, **25**(3), pp 236-243 (1988).
9. Lee, M. and Ho, C.M. "Lift force of delta wings", *Applied Mechanics Review*, **43**(9), pp 109-221 (1990).
10. Hummel, H. and Oelker, H.C. "Low-speed characteristics for the wing-canard configuration of the international vortex flow experiment", *Journal of Aircraft*, **31**(4), pp 868-878 (July-Aug. 1994)
11. Rae, H.W., Jr. and Pope, A., *Low-Speed Wind Tunnel Testing*, John Wiley & Sons, Inc. (1984)
12. Thomas, G.B., Roy, D.M. and John, H.L.V., *Mechanical Measurements*, Addison-Wesley Publishing Company (1993)
13. Nayebzade, A. "An experimental survey on the effects of canard position on the flowfield over the wing in subsonic flow", Msc. Thesis, Sharif University of Technology (Jan. 2008)

BIOGRAPHIES

Mohammad Reza Soltani, a professor in the aerospace engineering department of Sharif University of Technology, Tehran, has a PhD in aerodynamics from the University of Illinois at Urbana-Champaign, USA. His research interests include applied aerodynamics, unsteady aerodynamics wind tunnel testing, wind tunnel design, and data processing.

Farshid Askary graduated with a BS degree in aerospace engineering from Sharif University of Technology, from where he also received his MS in aerodynamics. His research interests include applied aerodynamics, unsteady aerodynamics wind tunnel testing, and data processing.

A.R. Davari is assistant professor in the department of mechanical and aerospace engineering at the science and research campus of the Islamic Azad University in Iran. He has conducted several experimental studies on unsteady aerodynamics and interference effects. He is also interested in new prediction and optimization methods in aerodynamics, such as neural networks and evolutionary algorithms. He graduated with a PhD degree in 2006 and has published over 11 journal papers since that time.

Arash Nayebzadeh graduated with a BS degree in aerospace engineering from Sharif University of Technology, from where he also received his MS in aerodynamics. His research interests include applied aerodynamics, unsteady aerodynamics wind tunnel testing, and data processing.